

AD-A114 046

EG AND G INC SALEM MA ELECTRONIC COMPONENTS DIV
NANOSECOND PULSER THYRATRONS.(U)
JAN 82 S FRIEDMAN

F/G 9/1

DAAK20-80-C-0282

ML

UNCLASSIFIED

DELET-TR-80-0282-2

For
APD 26

END
DATE
FILED
5-82
DTIC



(12)

Research and Development Technical Report
DELET-TR-80-0282-2

II

NANOSECOND PULSER THYRATRONS

AD A114046

Steven Friedman

EG&G, INC.
35 Congress Street
Salem, MA 01970

January 1982

Second Interim Report for Period 15 January 1981 — 30 July 1981

DISTRIBUTION STATEMENT

Approved for public release;
distribution unlimited.

Prepared for:
Electronics Technology & Devices Laboratory

ERADCOM

U.S. ARMY ELECTRONICS R&D COMMAND, FORT MONMOUTH, NEW JERSEY 07703



82 05 03 020

NOTICES

Disclaimers

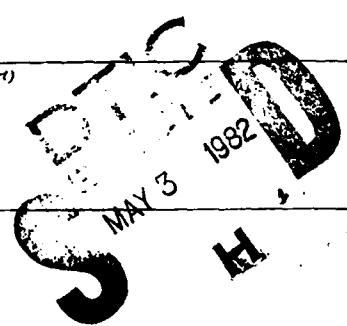
The citation of trade names and names of manufacturers in this report is not to be construed as official Government endorsement or approval of commercial products or services referenced herein.

Disposition

Destroy this report when it is no longer needed. Do not return it to the originator.

UNCLASSIFIED

SECURITY CLASSIFICATION OF THIS PAGE (When Data Entered)

REPORT DOCUMENTATION PAGE		READ INSTRUCTIONS BEFORE COMPLETING FORM
1. REPORT NUMBER DELEI-TR-80-0282-2	2. GOVT ACCESSION NO. AD-A114 CRL	3. RECIPIENT'S CATALOG NUMBER
4. TITLE (and Subtitle) Nanosecond Pulser Thyratrons	5. TYPE OF REPORT & PERIOD COVERED Second Interim 15 Jan 1981 - 30 July 1981	
7. AUTHOR(s) Steven Friedman	6. PERFORMING ORG. REPORT NUMBER DAAK20-80-C-0282	
9. PERFORMING ORGANIZATION NAME AND ADDRESS EG&G, Inc. 35 Congress Street Salem, MA 01970	10. PROGRAM ELEMENT, PROJECT, TASK AREA & WORK UNIT NUMBERS 62705 1L1 62705 AH94.01.03	
11. CONTROLLING OFFICE NAME AND ADDRESS Electronics Technology and Devices Lab (ERADCOM) ATTN: DELET-BG Fort Monmouth, NJ 07703	12. REPORT DATE January 1982	
14. MONITORING AGENCY NAME & ADDRESS (if different from Controlling Office)	13. NUMBER OF PAGES 43	
	15. SECURITY CLASS. (of this report) Unclassified	
16. DISTRIBUTION STATEMENT (of this Report) Approved for public release; distribution unlimited	15a. DECLASSIFICATION/DOWNGRADING SCHEDULE	
17. DISTRIBUTION STATEMENT (of the abstract entered in Block 20, if different from Report)		
18. SUPPLEMENTARY NOTES		
19. KEY WORDS (Continue on reverse side if necessary and identify by block number) Pulser Nanosecond Thyatron Circuit	Pulse Sharpener Capacitor	
20. ABSTRACT (Continue on reverse side if necessary and identify by block number) The fundamental feasibility of using thyatrtons for 1 ns turn-on of certain millimeter wave devices has been demonstrated, in that a voltage rise rate of 6 kv/ns has been achieved across a pure ~60 pF load. Use of ferrite bead saturable reactors enabled this to be accomplished at a thyatron pressure compatible with both reliable voltage holdoff and sufficiently short recovery time for a 20 kHz prr. The thyatron used was a 3-inch diameter HY-3013 modified for low inductance and designated HY-3013L. (Continued)		

DD FORM 1473 EDITION OF 1 NOV 68 IS OBSOLETE
JAN 73

UNCLASSIFIED

SECURITY CLASSIFICATION OF THIS PAGE (When Data Entered)

UNCLASSIFIED

SECURITY CLASSIFICATION OF THIS PAGE (When Data Entered)

20. Abstract (continued)

In particular this result shows that HY-3013L will meet the recently reduced EIO triggering requirements (\approx 3 kv), even though the ratio of load voltage to thyratron voltage will decrease to only 0.5-1.0 when the pulse width is reduced to 4 ns FWHM. (The exact value of this ratio will depend on the type of circuit employed.)

Operation at higher voltages will require a several-fold decrease in thyratron recovery time. Substantial reduction in thyratron jitter is also needed, and a reduction in the power required to trigger the thyratron would be desirable. Thyratrons based on the HY-3013L, but modified to achieve these goals, are being designed.

UNCLASSIFIED

ABBREVIATIONS AND SYMBOLS

A	Amperes (DC)
a	Amperes (pulsed)
C	Load capacitance
C_0	Storage capacitor capacitance
E_r	Thyatron reservoir voltage
EIO	Extended interaction oscillator
i	Current (instantaneous)
kv	Kilovolts (pulsed)
kV	Kilovolts (DC)
L	Total circuit inductance (including thyatron)
nF	Nanofarads
nH	Nanohenries
ns	Nanoseconds
p	Gas pressure
pF	Picofarads
prr	Pulse repetition rate
R	Load resistance
t	Time
t_f	Thyatron resistive fall time
t_r	Thyatron recovery time
τ_r	Load voltage rise time
μs	Microseconds
V	Load voltage
V_0	Initial storage capacitor voltage (thyatron voltage)
Z_0	Transmission line impedance
ϵ	Dielectric permittivity

Accession For	
<input checked="" type="checkbox"/> NTIS GRA&I	<input type="checkbox"/>
<input type="checkbox"/> DTIC TAB	<input type="checkbox"/>
Unannounced	<input type="checkbox"/>
Justification	
By _____	
Distribution/ _____	
Availability Codes	
Dist	Avail and/or Special
P	



Symbols used in Laplace transform circuit analysis and in component diagrams are defined as they appear.

TABLE OF CONTENTS

<u>Section</u>	<u>Page</u>
ABBREVIATIONS AND SYMBOLS.	iii
LIST OF ILLUSTRATIONS.	vii
1 FOREWORD	1
2 INTRODUCTION AND SUMMARY	3
3 EXPERIMENTAL RESULTS ON LOAD VOLTAGE RISE TIME	7
a. Effect of Saturable Reactors	7
b. Effect of Increasing Peak Load Voltage	7
4 CIRCUIT DESIGN FOR NARROW PULSE WIDTH AND HIGH REPETITION RATE.	13
a. Overall Circuit Design Considerations.	13
(1) T-Line Circuit.	14
(2) Lumped Circuit.	14
(3) Relative Advantages and Disadvantages of T-Line and Lumped Circuits.	15
(4) Experimental Results.	15
b. Load Design Considerations	16
c. Tentative Thyratron Housing Design	16
5 THYRATRON STATUS	21
a. Forward Voltage Holdoff.	21
b. Jitter and Triggering Requirements	21
c. Recovery Time.	24
d. Commutation Dissipation.	28
6 COLD CATHODE DEVELOPMENT	29
7 FUTURE PLANS	33
APPENDIX 1 CIRCUIT ANALYSIS	35

LIST OF ILLUSTRATIONS

<u>Figure</u>		<u>Page</u>
1	HY-3013L	5
2	Basic thyratron and load circuit	8
3	Saturable reactor section of circuit	9
4	Load voltage waveforms	10
5	Narrow load voltage pulse.	16
6	Liquid load for high prr	17
7	Thyratron housing cross section.	19
8	HY-3013L forward holdoff vs pressure	22
9	HY-3013L2.	23
10	Circuit for recovery time measurements	25
11	HY-3013L s/n 001 recovery time	27
12a	Impregnated cathode arc limit measurement.	31
12b	Cold oxide cathode arc limit measurement	31

1 FOREWORD

This is the Second Interim Technical Report for a program of research and development conducted under ERADCOM Contract DAAK20-80-C-0282 entitled "Nano-second Pulser Thyratrons," and covers the period 1 January 1981 to 30 July 1981.

The work described herein was performed by EG&G, Inc., Electronic Components Division, 35 Congress Street, Salem, Massachusetts 01970.

2 INTRODUCTION AND SUMMARY

The ultimate goal is to develop instant start thyratrons and circuits capable of switching millimeter wave devices at high speeds and repetition rates. During the past year, our efforts have concentrated on meeting the "Type II" requirements listed below:

	<u>Type II</u>
Peak Forward Voltage	6 kV
Peak Anode Current	360 amps
Pulse Rise Time (10-90%)	1.0 ns
Load Capacitance (including 50% stray capacitance)	60 pF
Burst Time	5-30 min
Off Time	120 min
Pulse Repetition Rate	20 kHz
Maximum Duty Cycle	2×10^{-4}
Life	1000 cycles
Jitter	100 picoseconds

As described in the First Interim Report, achieving these goals requires overcoming two fundamental difficulties. First, while a load voltage rise time τ_r of 1 ns requires extremely short thyratron commutation time and hence high pressure, 20 kHz prr requires fast thyratron recovery time and hence low to moderate pressure. Second, a 1 ns τ_r demands very low circuit inductance, on the order of 10 nH.

These difficulties have been overcome to the extent that basic project feasibility has been demonstrated. A circuit was constructed having sufficiently low inductance so that thyratron commutation time was the limiting factor in the load voltage rise rate. This limitation was then partially overcome by use of saturable reactors in the form of ferrite beads. Finally, by allowing the peak load voltage to be 10 kv instead of 6 kv, a 10-90% rise time of 1 ns was obtained across ~60 pF for the last 6 kv of the voltage waveform.* This was accomplished while operating the thyratron at a pressure

*In the final application, the first 4 kv constituting the slow rising portion of the waveform can be prevented from affecting the millimeter wave device by simply reducing the pedestal voltage by 4 kv.

low enough to be consistent with 20 kHz prr (50 μ s recovery time). The thyratron voltage was 6 kv.

This result shows that the thyratron used (HY-3013L, Figure 1) can meet the recently reduced EIO trigger requirements (\leq 3 kv), even though the ratio of load voltage to thyratron voltage will decrease to only 0.5-1.0 when the pulse width is reduced to 4 ns FWHM. (The exact ratio will depend on the type of circuit used, as discussed in Section 4.)

Operation at higher voltages will require a several-fold decrease in thyratron recovery time. Substantial reduction in jitter is also needed, and a reduction in the power required to trigger the thyratron is desirable.

Commutation dissipation has been reassessed using theory applicable to high current rise rates, and at 20 kHz will be severe unless greatly reduced by the saturable reactors.

The problems of recovery time, jitter, and trigger power should be solvable by straightforward modifications in thyratron design.

Planning has begun on a modulator to evaluate thyratrons and saturable reactors under high prr conditions. Modulator construction, and subsequent thyratron evaluation, will involve substantial effort, and it is not clear what thyratron design changes, if any, will ultimately be required.

Another area investigated was the development of a cold cathode. Preliminary experiments with barium aluminate impregnated tungsten show this material to be capable of meeting the peak current requirements of this project.

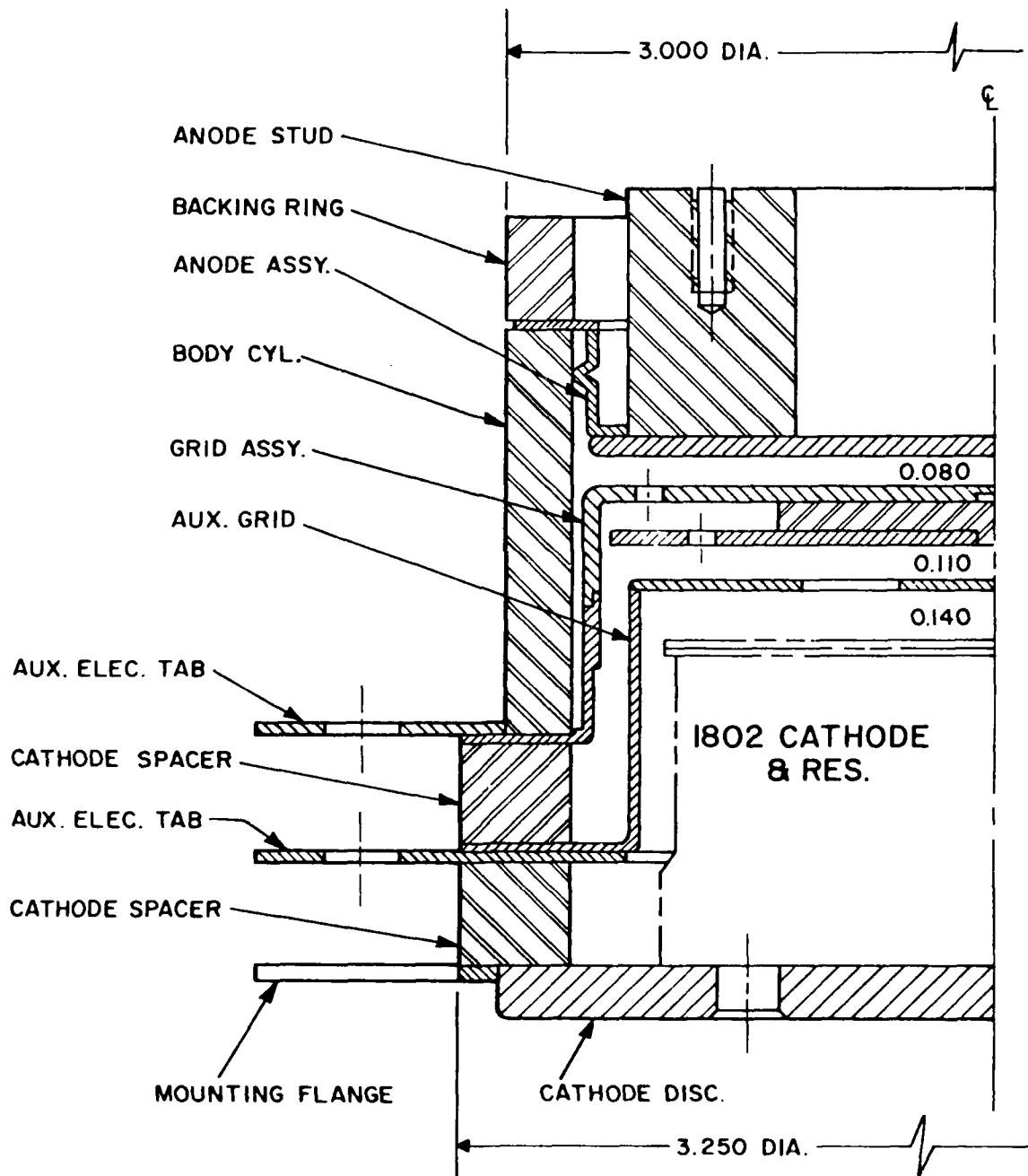


Figure 1. HY-3013L (low inductance HY-3013).

3 EXPERIMENTAL RESULTS ON LOAD VOLTAGE RISE TIME

a. Effect of Saturable Reactors

The basic circuit, without saturable reactors, is shown in Figure 2. Load voltage waveforms obtained with this circuit were analyzed using the numerical theory described in the First Interim Report, pp. 23 ff. (This analysis is described in detail in Monthly Status Report No. 6.) The main conclusion was that the load voltage rise time (2.5-3 ns) was being limited by the resistive fall time (commutation time), of the thyratron and that saturable reactors would therefore be required.

Saturable reactors were introduced into the circuit as shown in Figure 3. Eleven ferrite beads (Ferroxcube Type 4A6) were mounted in series with the 5 nF capacitor on a 0.045-inch diameter rod. The load capacitance (45 ± 10 pF) now included the ferrite section.

Figures 4a and 4b show load voltage waveforms $V(t)$ with and without ferrite beads. The reservoir voltage E_r was 6.0 V, corresponding to 0.7 torr; prr was 10 Hz, and the thyratron voltage V_0 was 6 kv.

The maximum dV/dt with the ferrites was about 4.8 kv/ns. Without ferrites, E_r had to be increased to 7.0 V (0.95 torr) to achieve a comparable dV/dt (see Figure 4c).

Operation at $E_r = 6.0$ V enables the thyratron HY-3013L to achieve reliable 6 kv holdoff, and recovery within the 50 μ s required for 20 kHz operation as shown in subsection 5.c.

b. Effect of Increasing Peak Load Voltage

The major difficulty in charging the capacitive load to 6 kv in 1 ns is that the early part of the voltage rise is always slow compared to the main part. Ferrites reduce thyratron commutation effects, but, even in a circuit having an ideal switch, the theoretical load voltage would be proportional to $1 - \cos \omega t$, and hence start off slowly.

If the output power of the millimeter wave device being triggered does not reach a significant level until the applied voltage comes within 6 kv of its maximum value, V_m , then, in principle, the above problem can be avoided by reducing the pedestal voltage so that the slow early part of the sliver is more than 6 kv below V_m .

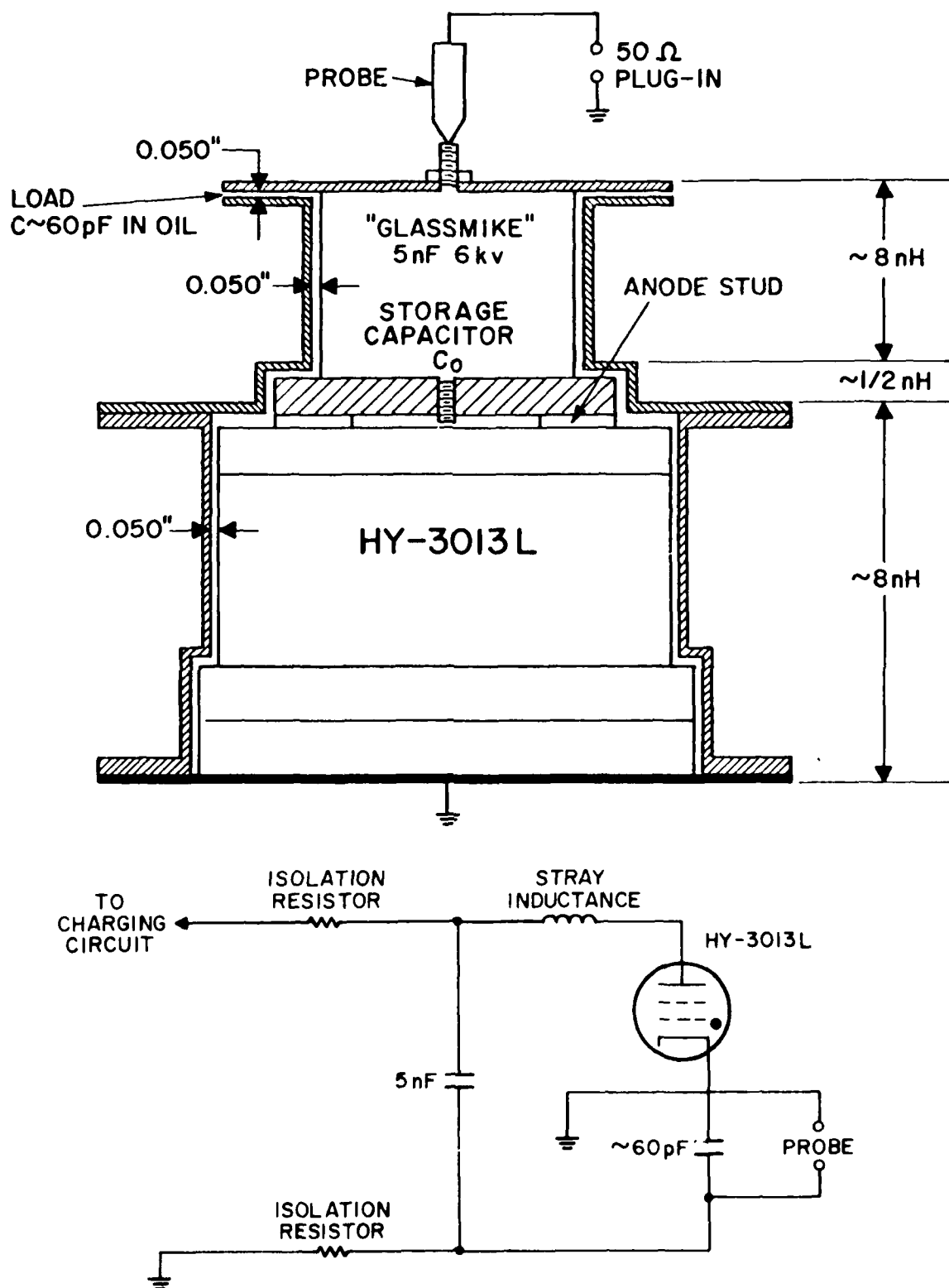


Figure 2. Basic thyratron and load circuit.

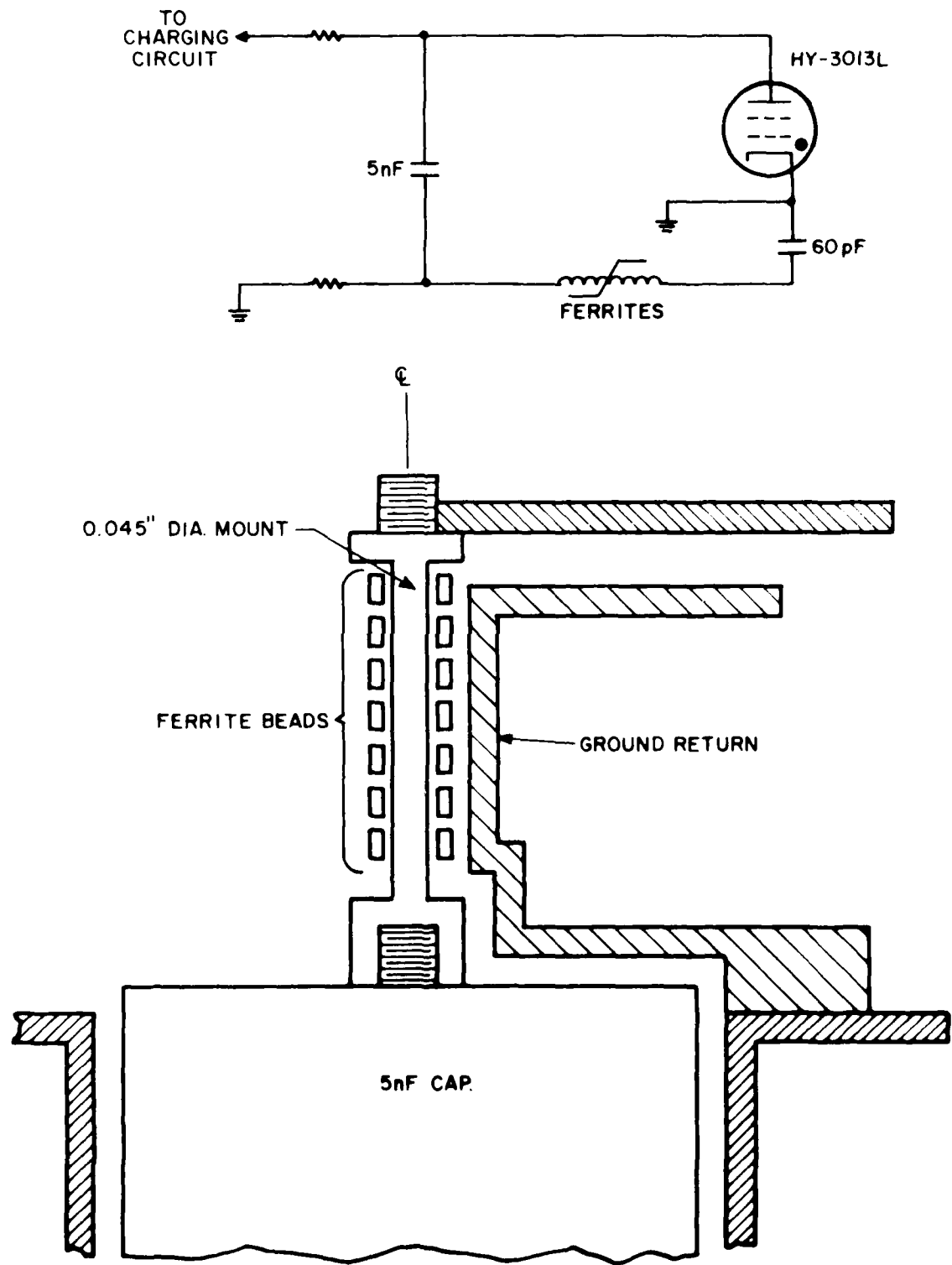


Figure 3. Saturable reactor section of circuit.

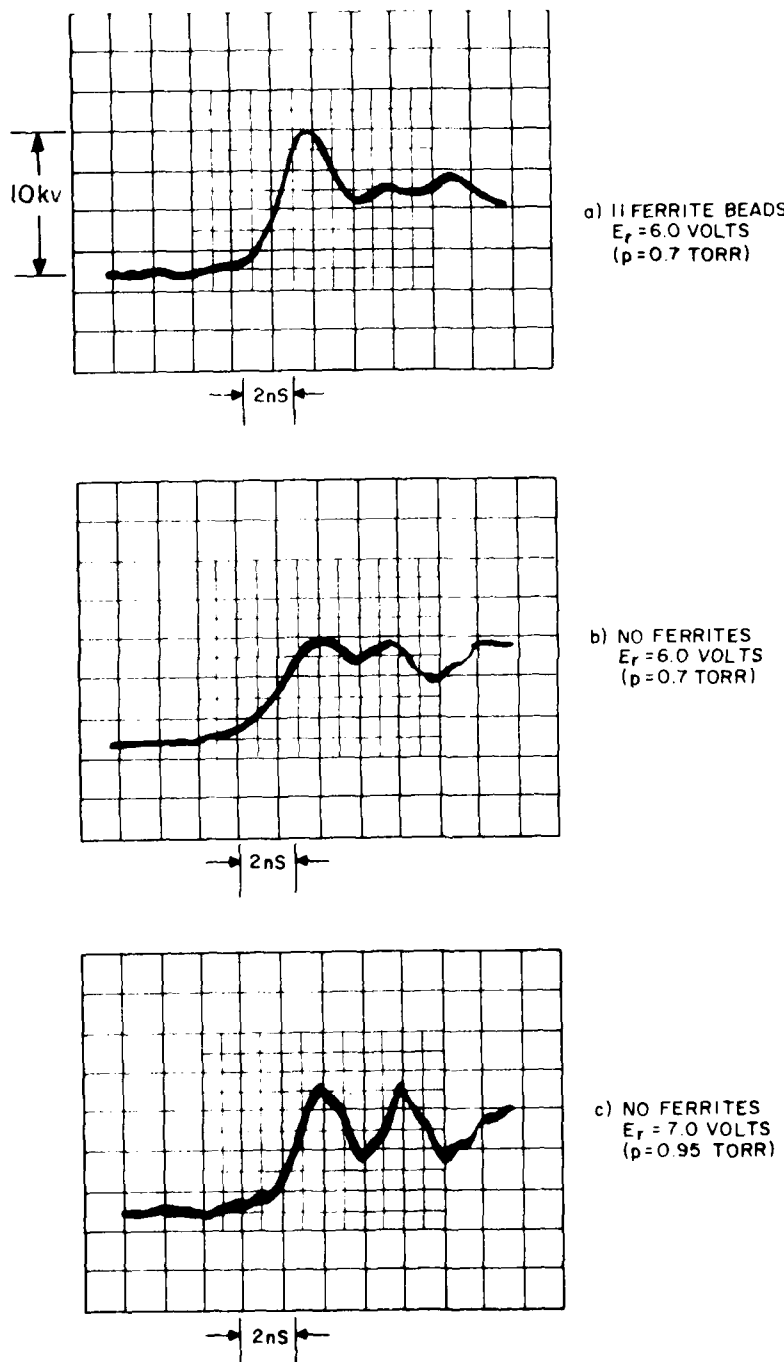


Figure 4. Load voltage waveforms.

In Figure 4a, for example, the peak voltage is 10 kv, the time to cover the last 6 kv is 2 ns, and the 10-90% rise time for the last 6 kv (the time to go from 4.6-9.4 kv) is 1 ns.

Thus, given a millimeter wave device that goes from off to on over a 6 kv interval, the present modulator could switch such a device on in 1 ns, while operating at a V_0 of 6 kv and a thyratron pressure low enough to achieve 20 kHz.

The theory and the circuit problems involved in narrowing the load voltage pulse to 4 ns FWHM are discussed in Section 4, and implications for thyratron design are considered in Section 5.

4 CIRCUIT DESIGN FOR NARROW PULSE WIDTH AND HIGH REPETITION RATE

In Section 3, experimental results were discussed pertaining to switching on a millimeter wave device in 1 ns. The problem was considered to be equivalent to charging a purely capacitive load. No consideration was given as to how the load voltage pulse was to be terminated in the required 4 ns, thus creating an idealized condition, in that the maximum voltage V_m appearing across the load after the thyratron fired was greater than the initial charging voltage V_0 on the thyratron.* It was only necessary for V_0 to be 6 kv in order for V_m to be 10 kv. Given this, it was demonstrated that a 60 pF millimeter wave device could be turned on in 1 ns while operating the thyratron at a voltage and pressure compatible with a good holdoff and 20 kHz operation.

Now the effects introduced by the necessity of turning off the millimeter wave device 4 ns after turn-on (i.e., the applied voltage pulse should have a 4 ns FWHM) must be considered.

Pulse termination by crowbarring is unfeasible at this time due to switch closure time, jitter, weight and volume considerations, thus leaving termination via RC decay where R is a resistance placed across the load capacitance. The subsequent effect will be to substantially reduce V_m/V_0 , thus requiring the thyratron to sustain a larger V_0 .

Power dissipation at high prr must also be considered, particularly in the design of the load.

The types of circuits and components being considered for construction, along with tentative parameter values, are discussed in the following subsections.

a. Overall Circuit Design Considerations

Two types of circuits are being considered: transmission line and lumped. These are diagrammed schematically and analyzed mathematically in Appendix 1. First, each circuit is discussed, and then their relative advantages and disadvantages are compared.

*This was due to the action of stray inductance between C_0 and C. In essence, Figure 2 is a resonant charging circuit in which the stray inductance, as well as thyratron inductance, acts as a charging choke.

(1) T-Line Circuit

The T-line will have a two-way transit time of 3 ns, and load resistor R will be chosen so that the 60 pF load capacitor C discharges with an e-folding time of 1 ns. R and Z_0 will be made equal to avoid reflections,* and the thyratron will be housed so as to present an impedance Z_0 .

Inductance L must be low enough to yield the desired 1 ns load voltage rise time. Setting $R = Z_0$ and $C = 60 \text{ pF}$ in Appendix 1A gives $L \approx 3 \text{ nH}$, $R = Z_0 = 15 \text{ ohms}$. The capacitor discharge time is then $RC = 0.9 \text{ ns}$.

Although the inductance requirement is very stringent, a somewhat larger value should be tolerable, because the above parameter values were derived assuming perfect critical damping, whereas in practice a small amount of ringing is allowable. Thus, a satisfactory load voltage waveform should be obtainable over a range of circuit parameters. This is demonstrated experimentally in the lumped circuit case below. Furthermore, as discussed earlier, it may not be necessary to achieve a 1 ns rise time in order to get 6 kv/ns across the load if the maximum load voltage is allowed to be somewhat higher.

Saturable reactors will be mounted around the center conductor of the T-line.

A Blumlein configuration is also being considered, since this would result in a theoretical V_m/V_0 of 1, substantially easing the thyratron recovery problem (see Section 5). The increased space, weight, and complexity of a Blumlein may be insignificant.

(2) Lumped Circuit

The load voltage for the critically damped case is derived in Appendix 1B. Storage capacitance C_0 , load resistance R, and inductance L are all determined by the 4 ns FWHM criterion to be $C_0 = 480 \text{ pF}$, $R = 6.5 \text{ ohms}$, $L = 9 \text{ nH}$. The inductance here includes the thyratron, load, saturable reactors, and connections.

*Actually, some reflection will be required to re-set the saturable reactors.

(3) Relative Advantages and Disadvantages of T-Line and Lumped Circuits

The main advantages of the T-line circuit are that the inductance of the switch and saturable reactors can be incorporated into Z_0 , and the pulse width can be corrected if necessary simply by changing the length of the line.

The lumped circuit is more compact and simple to construct than the T-line. It theoretically allows a higher ratio of load voltage to thyratron voltage ($V/V_0 = 0.7$ vs 0.5 for the T-line), but this advantage is offset somewhat by the higher current requirements due to R being lower.

Two significant points bear on evaluation of the T-line:

- 1) T-line theory is only accurate when the pulse width is much greater than the rise time. Since the expected ratio of 3 to 1 is borderline, a lumped circuit is created if the voltage is increased and a rise time of 2 ns is set.
- 2) Successful operation depends on whether or not the thyratron section can be made to resemble Z_0 . Since the current distribution inside the tube is likely to be complex for such short pulses, this may be difficult to do.

(4) Experimental Results

A lumped circuit was constructed using thyratron HY-3013L, the existing ferrite mount, and a few small disc capacitors wrapped in aluminum foil to provide a low inductance return path. The load consisted of four 110 ohm carbon resistors soldered in parallel across 47 pF. C_0 was 220 pF, and V_0 was kept to 3 kv because no oil insulation was used. L was estimated to be ~100 nH.

The resulting load voltage pulse is shown in Figure 5. The FWHM was 10 ns, and the peak voltage 1.7 kv = 0.57 V_0 .

Two points are clear. First, the pulse is nicely damped even though the circuit parameters only crudely satisfy the theoretical criteria for critical damping. Second, it would be desirable for the thyratron to be able to hold off double the required peak load voltage, even though lumped circuit theory predicts $V_{max}/V_0 = 0.7$.

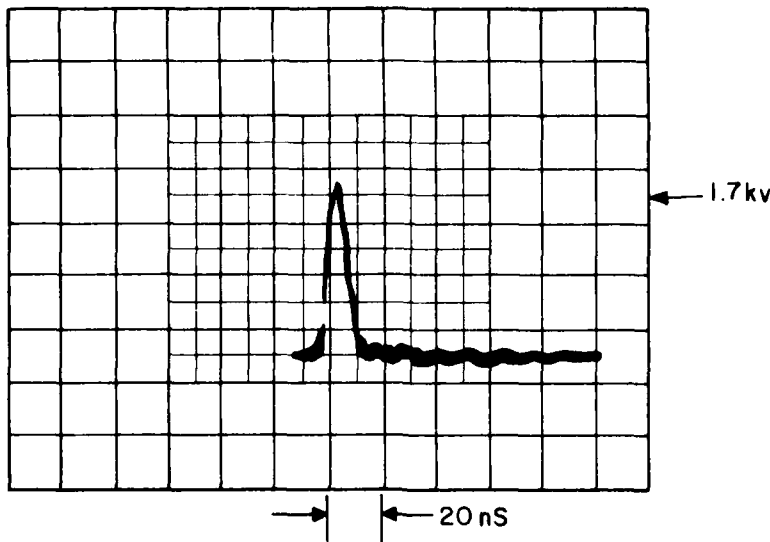


Figure 5. Narrow load voltage pulse.

b. Load Design Considerations

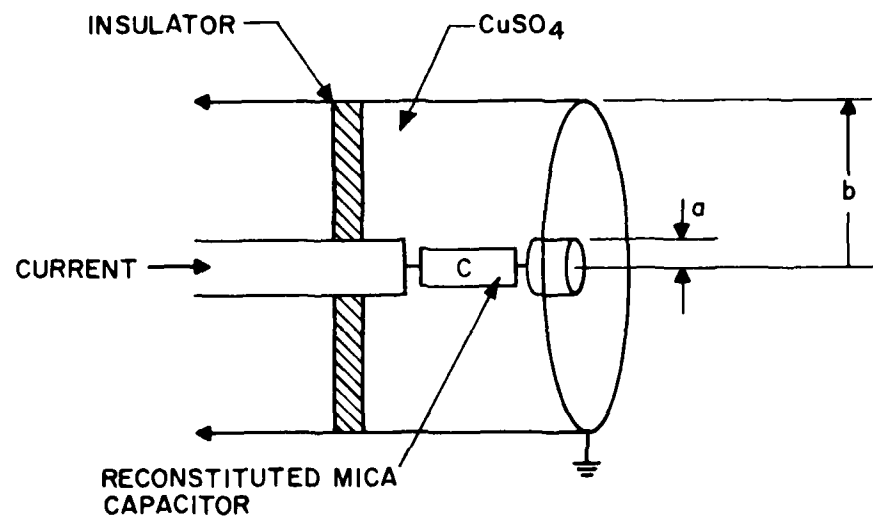
The average power dissipated in the load resistor is expected to be at least 100 watts, and in the worst case as much as 1 kW. (The worst case would be a lumped circuit attaining a 6 kv/ns load voltage pulse by impressing 10 kv across a 6.5 ohm load resistor.) It is unlikely that this could be tolerated by any solid resistor small enough to have a suitably low inductance. This is especially true considering that the skin effect will result in this power being deposited in a small fraction of the total volume. Skin effect also would make the effective value of R difficult to control.

Therefore, a liquid load (copper sulfate solution), shown in Figure 6, will be used. Because of its high dielectric constant (around 80), we expect a significant contribution to the load capacitance to be made by the "resistor." In fact, we may not use any additional capacitors at all (Figure 6).

c. Tentative Thyratron Housing Design

To model the thyratron in the manner of a coaxial line, two simplifying assumptions will be made:

- 1) The discharge fills the entire volume of the thyratron.
- 2) The dielectric constant of ceramic is approximately 9.



$$C_{\text{Total}} = C + \frac{2\pi\epsilon}{\ln \frac{b}{a}} = C + \frac{45}{\ln \frac{b}{a}} \text{ pF/cm for CuSO}_4 \quad (\epsilon/\epsilon_0 = 80)$$

Since $\frac{b}{a}$ must be small for low inductance, C may not be needed to get a 60 pF load capacitance.

Figure 6. Liquid load for high prr.

The thyratron is considered to be directly centered within the current-return cylinder, so the total capacitance of the thyratron housing can be viewed as two components in series; the capacitance from the outer edge of the discharge to outer edge of the ceramic, and the capacitance from outer edge of the ceramic to the current-return cylinder. The radius of the current-return cylinder can then be calculated as follows:

The radius of the discharge (for a 3-inch tube) will be taken to be 1.25 inches. The outer radius of the ceramic is 1.5 inches. The capacitance arising from the ceramic dielectric is therefore

$$\frac{2\pi(9)(8.85 \times 10^{-12})}{\ln(\frac{1.5}{1.25})} = 2.74 \text{ nF/meter} \quad (1)$$

The capacitance from ceramic to the current-return cylinder (radius "b") is given by

$$\frac{2(8.85 \times 10^{-12})}{\ln(\frac{b}{1.5})} = \frac{0.056}{\ln(\frac{b}{1.5})} \text{ nF/meter} \quad (2)$$

The inductance of the thyratron housing is given by

$$50(1 + 4 \ln[b/1.25]) \text{ nH/meter} \quad (3)$$

so that, in order to have an impedance of 15 ohms, the total housing capacitance must be

$$\frac{50}{225}(1 + 4 \ln[b/1.25]) \text{ nF/meter} \quad (4)$$

Adding (1) and (2) in series to get (4) gives an equation for the housing radius b:

$$\frac{1}{2.74} + \frac{\ln(b/1.5)}{0.056} = \frac{225}{50(1 + 4 \ln[b/1.25])} \quad (5)$$

Solving for b gives $b \approx 1.65$ inches. This results in a narrow annulus between the thyratron and current return ($1.65 - 1.50 = 0.150$ inch). Filling the annulus with electrically insulating material may be required. Assuming this material has a dielectric constant 3 (as do transformer oil, kapton, and many others) changes the above calculation to give $b \approx 1.9$ inches.

Figure 7 illustrates a tentative thyratron housing design with pertinent dimensions.

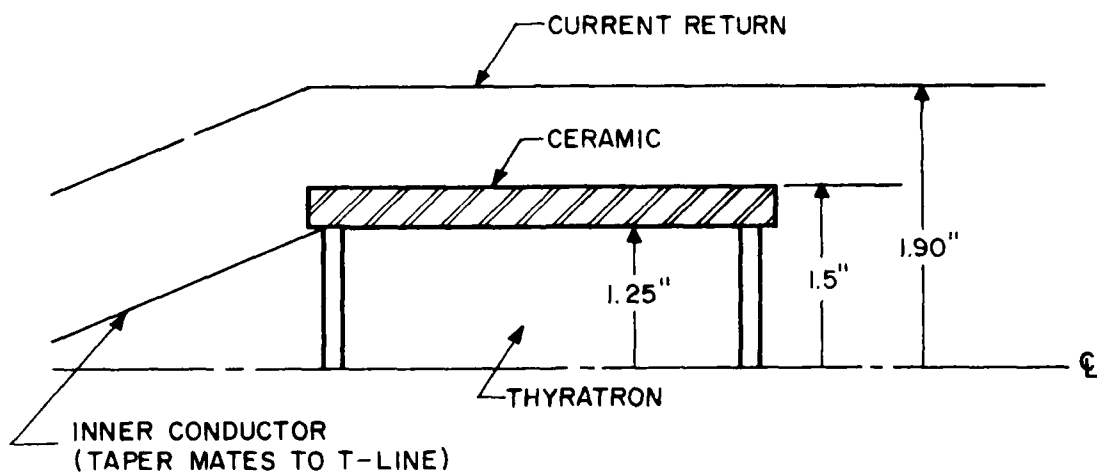


Figure 7. Thyratron housing cross section.

5 THYRATRON STATUS

The mildest voltage condition under which the thyratron would have to operate is the one consistent with the recently reduced E10 trigger requirements, i.e., a trigger voltage $\gtrsim 3$ kv. V_0 would need to be around 3 kv for a Blumlein circuit, and around 6 kv for a single T-line or lumped circuit.

In the worst case, a peak load voltage of 10 kv would be required (as in Figure 4a), and therefore $V_0 = 20$ kv.

The thyratron presently in use, HY-3013L, is limited by recovery time to only the mildest condition. Proposed design changes to extend its capabilities are described below.

a. Forward Voltage Holdoff

A plot of forward holdoff (dynamic breakdown voltage, DBV) vs pressure for HY-3013L is shown in Figure 8. The applied voltage waveform is shown inset; it has a 4 μ s rise time and a 2 μ s dwell. Since sufficiently fast load voltage rise rates have been obtained without exceeding 0.7 torr, HY-3013L holdoff is satisfactory as is.

It is nevertheless worthwhile to see if holdoff can be extended to even higher pressures, since this would reduce commutation dissipation and further increase the load voltage rise rate. To this end, thyratron HY-3013L2 (Figure 9) is being constructed with narrower grid slots and a reduced grid-anode space.

b. Jitter and Triggering Requirements

The jitter was measured to be 2-3 ns, based on the time between application of the trigger pulse to the control grid and the appearance of the commutation spike on the grid current waveform. The thyratron was triggered using a 500 V, 6 ohm driver, with about 100 mA keep-alive to the auxiliary grid; prr was 10 Hz.

When the trigger power was reduced by employing a TM-29 (1400 V, 100 ohms), jitter increased to 10-15 ns. With a TM-27 (800 V, 200 ohms), the tube failed to trigger altogether.

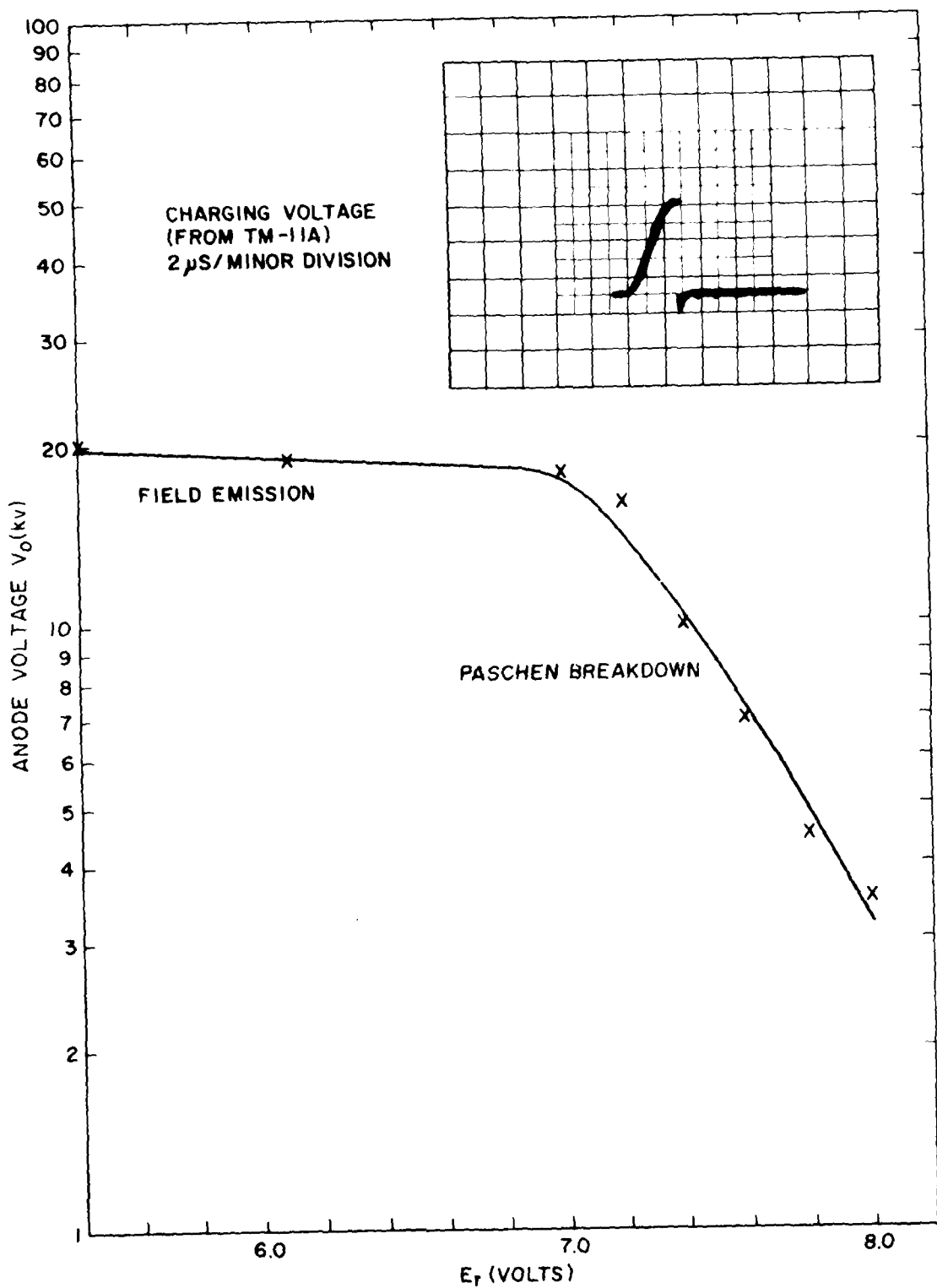
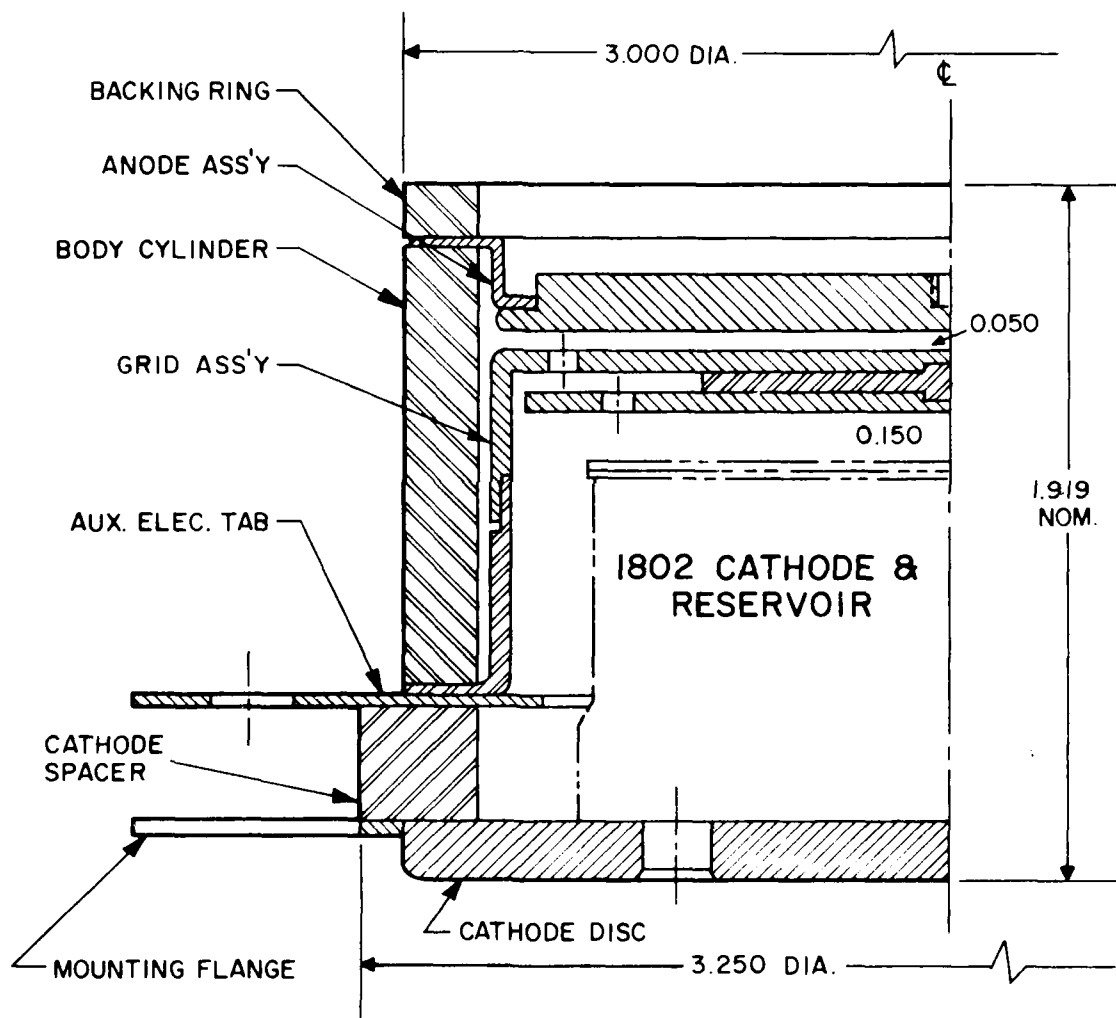


Figure 8. HY-3013L forward holdoff vs pressure. (Grid-anode space = 0.080 inch.)



Note:

- (1) Grid and baffle slots annular 0.060 inch wide.

Figure 9. HY-3013L2.

Since a standard HY-3013 has less than 2 ns jitter using a TM-29, and can be triggered (although not reliably) using a TM-27, it is clear that HY-3013L has a triggering problem. Evidence from the behavior of the HY-8 thyratron suggests that triggering would be eased and jitter reduced by bringing the control grid slots, auxiliary grid slots, and cathode into closer alignment, thus enabling the discharge to follow a less tortuous path.

The HY-8 has been reported to have exceptionally low jitter, on the order of 60 ps. The offsets between auxiliary grid, grid baffle, and control grid slots for this tube are only 0.025 inch, as compared to 0.250 inch and 0.080 inch for the HY-3013L.

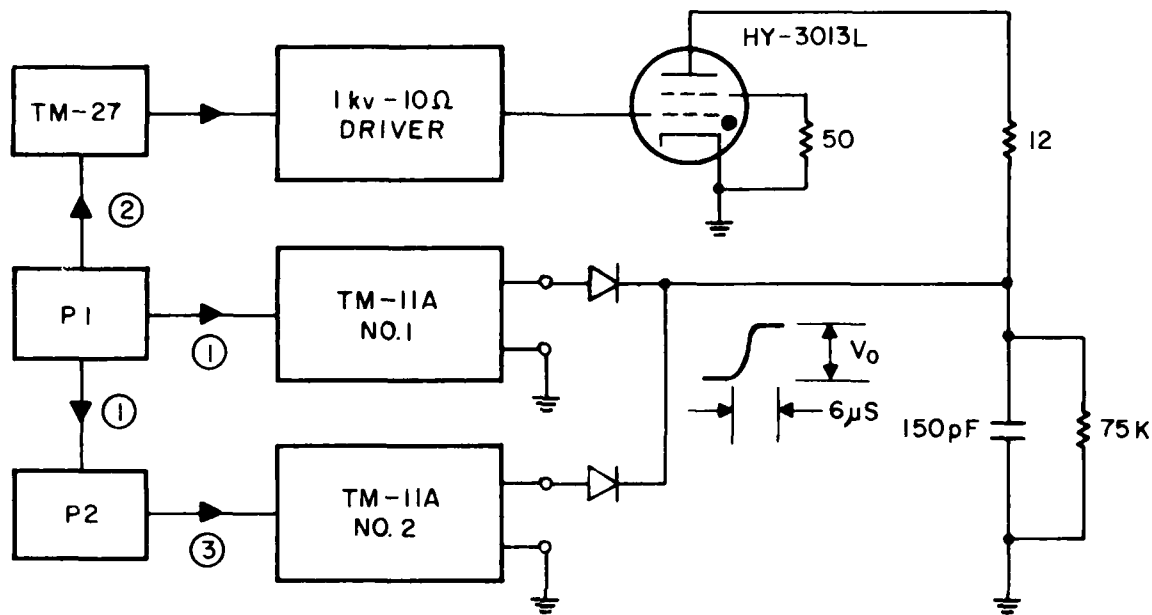
HY-3013L2, presently under construction, is a triode, and is therefore expected to require very little trigger power; a TM-27 should suffice, and a 20 kHz TM-27 already exists in-house.

A drawback of HY-3013L2 is that, being a triode, keep-alive cannot be used to reduce jitter. However, the combination of high pressure and easy triggerability should result in jitter being lower than usual.

c. Recovery Time

Operation at 20 kHz implies a recovery time t_r of 50 μ s or less. While thyratrons operating at standard pressures (0.2-0.3 torr) can achieve this routinely, the need here for fast commutation time and high current rise rate dictates triple these pressures. Since thyratrons recover primarily by diffusion of charged species to walls and electrode surfaces, recovery time increases with pressure. t_r also increases with current, and therefore with V_0 .

Recovery time measurements for HY-3013L made at $V_0 = 6$ kv were reported in the First Interim Report. At this voltage, t_r remained below 50 μ s up to a pressure of 0.9 torr, a pressure sufficiently high to allow a 6 kv/ns load voltage rise rate. Recently, measurements of t_r have been made at higher V_0 . The elimination of the series charging triode in the circuit used (Figure 10) represented an improvement over the circuit used to obtain the earlier data. The frequent failure of this triode to recover had caused circuit operation to be erratic, making accurate t_r measurements difficult. In the new circuit, V_0



Sequence of Events:

- (1) Pulser P1 triggers TM-11A No. 1, which charges 150 pF to V_0 . Simultaneously P1 triggers P2.
- (2) A delayed pulse from P1 triggers TM-27 which in turn triggers a 1 kV-10 Ω driver, which triggers HY-3013L about 2 μ s after the 150 pF reaches V_0 .
- (3) Some time after HY-3013L fires, P2 triggers TM-11A No. 2, re-charging 150 pF to V_0 , provided the time interval between (2) and (3) is greater than the HY-3013L recovery time.

Recovery was fastest for the triggering arrangement shown.

Figure 10. Circuit for recovery time measurements.

pulses were supplied by two production TM-11A trigger units fired in succession. As before, the thyratron was triggered at the crest of the first pulse only, and t_r was determined by how soon afterward the second V_0 pulse could be applied without the thyratron commutating a second time. (See First Interim Report, pp. 13 ff.) Two TM-11A units were necessary to simulate 20 kHz operation, because each one was only capable of operating up to 100 Hz.

It is important to note that double-pulsing a thyratron in this manner is not entirely equivalent to running at high prr. Since the time interval between pulse pairs is long, the tube remains cool so that metal vapor does not build up, and temperature gradients that can cause the discharge to alter its path cannot arise. Also, static charges on the ceramic have time to leak away. At true high prr, these effects accumulate, and can degrade recovery.

Results for t_r vs V_0 at several pressures are plotted in Figure 11. Note that at higher pressure there is a value of V_0 at which t_r increases sharply, and that this value is not much beyond 6 kv.

Attempts to reduce t_r by application of negative bias either had no effect, or resulted in failure of HY-3013L to commute. The tube's poor triggerability (discussed above) prevented operation in a regime where negative bias would have been effective in reducing t_r .

Increasing the resistance in series with HY-3013L from 12 ohms to 100 ohms reduced t_r at higher V_0 , but results were erratic.

Further experimentation with more readily triggerable thyratrons (HY-3013L2) is needed to reliably establish the minimum achievable recovery time. However, changes in thyratron design will be required to achieve $t_r < 50 \mu s$ for $V_0 > 10$ kv.

Since recovery is a diffusion process, and therefore varies as distance squared, some straightforward ways to reduce t_r are: 1) reduce the inter-electrode spacings, 2) reduce the volume between the control grid and baffle, and 3) eliminate the control grid-baffle space altogether by making the control grid a single thick electrode, with its slots angled to eliminate line of sight between cathode and anode.

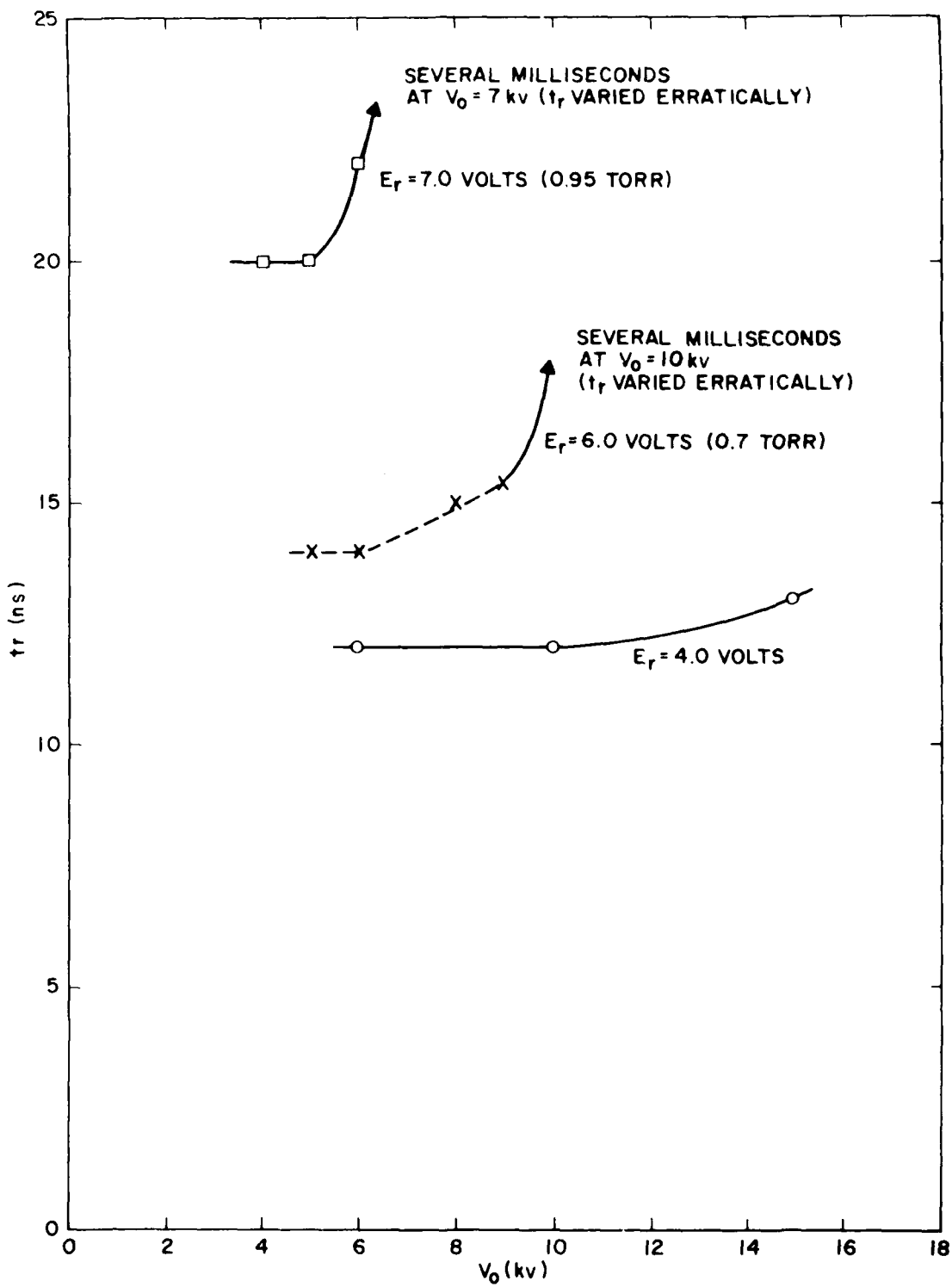


Figure 11. HY-3013L s/n 001 recovery time.

d. Commutation Dissipation

A 20 kHz operating rate, coupled with short current rise times, will cause large commutation dissipation at the thyratron anode. This dissipated power is proportional to the quantity Πb , defined by

$$\Pi b = V_0 \times prr \times di/dt$$

Πb ratings for thyratrons have recently been developed to replace the old Pb ratings, which were valid only for current rise rates below 5×10^{10} amps/sec.

In this application, Πb may be as high as 10^{20} . This exceeds the accepted safe value for 3-inch diameter thyratrons by 3 orders of magnitude. The use of ferrites is expected to greatly reduce the commutation dissipation, but by how much is not known. Since only air cooling can be utilized, it is imperative that tests be conducted to measure the anode dissipation.

It is not clear that going to larger diameter thyratrons will alleviate this problem, since the pulse length is so short that the discharge has little time to spread. Therefore, 3-inch diameter tubes will continue to be used for the present.

6 COLD CATHODE DEVELOPMENT

Cathodes made from barium aluminate impregnated tungsten have shown great promise as cold cathodes. They can sustain high current densities without arcing even when cold, and can withstand arcs that do occur without deterioration of their emitting properties, thus enabling cathodes of small size, and hence ultra-low inductance (less than 1 nH) to be built.

The threshold cathode current density for cold cathode arcing was measured to be 80 a/cm^2 for $10 \mu\text{s}$ pulses. This measurement was performed as part of the Instant Start Thyratron Program at EG&G. For the Nanosecond Pulser Project, shorter pulses were of interest. A production 3-inch diameter tetrode thyratron with a flat 10 cm^2 slab of impregnated tungsten in place of the usual oxide coated vanes was therefore retrofitted and operated in a low inductance circuit.

The thyratron was an HY-3004, a tetrode version of the HY-1802, and is also the tube from which the HY-3013 design was originally derived.

The test circuit provided sinusoidal current pulses of about 75 ns FWHM and peak currents up to 6 ka at $V_0 = 10 \text{ kv}$, limited by flashover between the tube and current return shroud. Since detection of arcing relies on observing sudden drops in grid voltage, it would have been better had a flat-topped current pulse been available to avoid inductive contributions to the voltage. However, a low inductance PFN large enough to provide such a pulse at the low impedance levels desired was unavailable, given that the HY-3004 is a fairly inductive tube, making for slow current rise times. To avoid this difficulty, the impregnated cathode tube grid voltage waveform was compared with that of a standard oxide cathode HY-3004 in the same circuit.

The grid voltage waveform during commutation of the impregnated cathode tube is shown in Figure 12a. prr was 5 Hz, and several minutes of operating time was accumulated. The waveform was independent of cathode temperature, and was virtually identical to that obtained with the hot oxide cathode HY-3004. The data shown were taken at a peak current of about 6 ka, corresponding to 60 a/cm^2 for the oxide cathode and 1000 a/cm^2 for the impregnated cathode.

When the oxide cathode was operated cold, the grid voltage waveform changed to that shown in Figure 12b. Whether or not this represents arcing is unclear. While the early drop in grid voltage implies arcing, the good shot-to-shot reproducibility of the waveform, coupled with the observation that it was only seen when the keep-alive current exceeded a certain value (about 50 mA), suggests that some other type of abnormality was occurring.

We conclude that for pulse lengths on the order of 100 ns or less, at low average power, impregnated cathodes can sustain current densities in excess of 1 ka/cm^2 without arcing, even when cold. The theoretical arc limit for hot oxide cathodes under these conditions is about 200 a/cm^2 . (Creedon et al., 7th Symp. on Hydrogen Thyratrons and Modulators, Ft. Monmouth, New Jersey, 1962.)

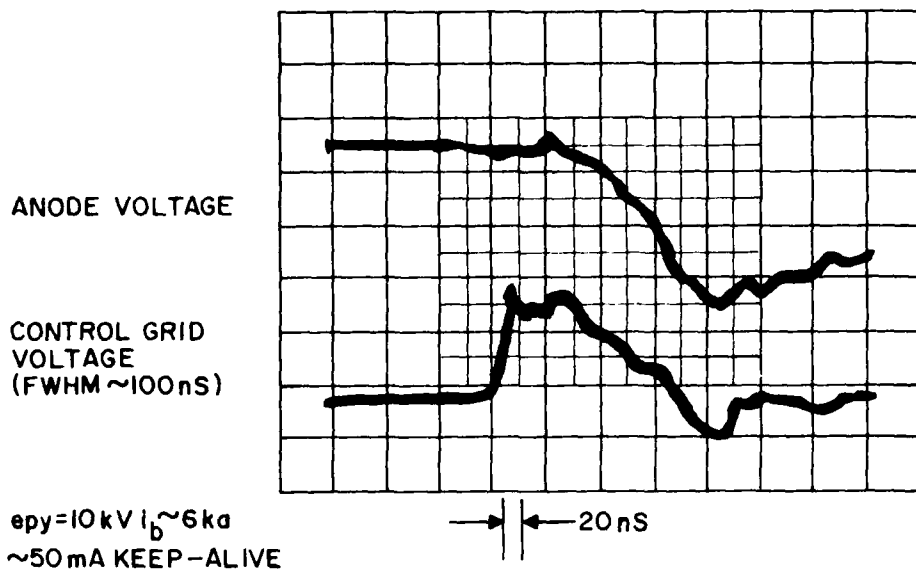


Figure 12a. Impregnated cathode arc limit measurement. (Same waveforms obtained with both hot and cold cathode.)

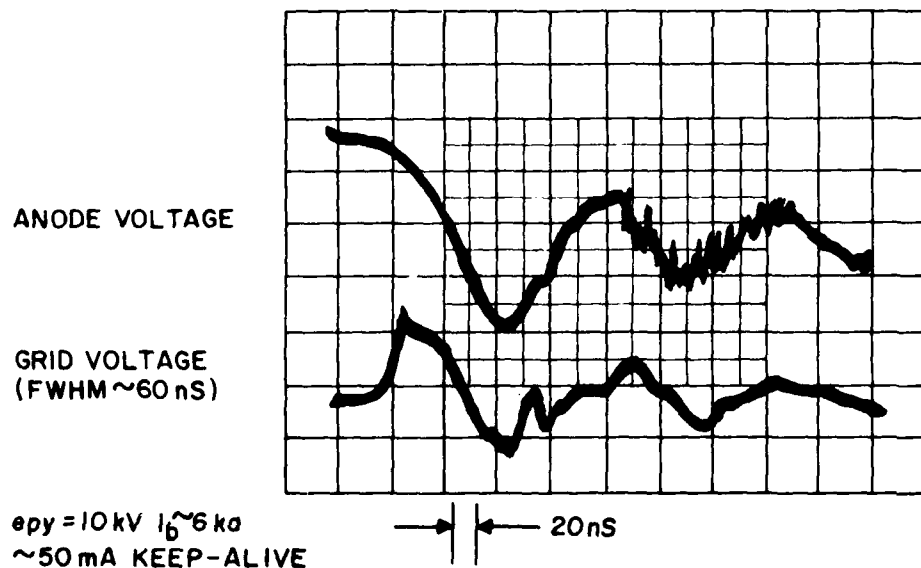


Figure 12b. Cold oxide cathode arc limit measurement.
Typical "arc" waveform.

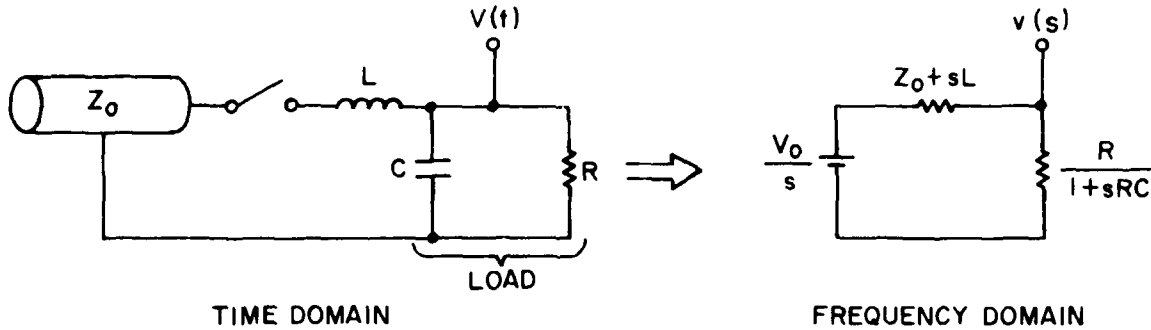
7 FUTURE PLANS

Construction of a multi-kHz modulator, with a goal of 20 kHz, is being given high priority since commutation dissipation measurements are crucial to determining the feasibility of 20 kHz operation.

Thyatron HY-3013L2, designed for better holdoff and easier triggering, will be completed and characterized. The resulting information will be used to help design future high-holdoff, fast recovery, low-jitter thyatrons, preliminary plans for which are already underway.

APPENDIX 1
CIRCUIT ANALYSIS

A. T-LINE ANALYSIS



$$\frac{v(s)}{V_0} = \frac{1}{s} \frac{1}{1 + \frac{Z_0}{R} + sCZ_0 + s \frac{L}{R} + s^2 LC} \quad (A-1)$$

$$LC \frac{v(s)}{v_0} = \frac{1}{s} \frac{1}{s^2 + s \left(\frac{Z_0}{L} + \frac{1}{RC} \right) + \frac{1 + Z_0/R}{LC}} \quad (A-2)$$

For critical damping, this should have the form

$$\text{LC} \frac{v(s)}{V_0} = \frac{1}{s} \cdot \frac{1}{(s + \alpha)^2} = \frac{1}{\alpha^2} \left[\frac{1}{s} - \frac{1}{s + \alpha} - \frac{\alpha}{(s + \alpha)^2} \right] \quad (\text{A-3})$$

(Partial fraction expansion)

This requires that " α " satisfy two conditions:

$$2\alpha = \frac{Z_0}{L} + \frac{1}{RC}, \quad (A-4)$$

$$\alpha^2 = \frac{1 + Z_0/R}{LC} \quad (A-5)$$

Then

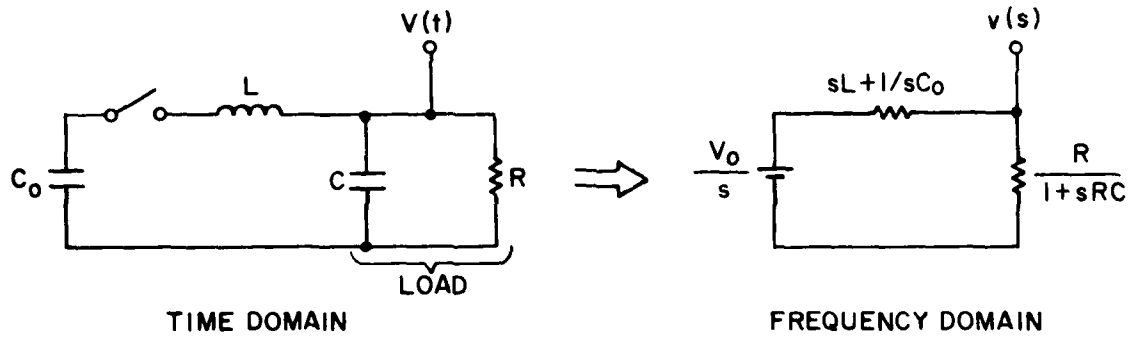
$$\frac{v(t)}{V_0} = \frac{R}{R + Z_0} \left[1 - e^{-\alpha t} - \alpha t e^{-\alpha t} \right]$$

The 10-90% rise time is $\tau_r = \frac{3.5}{\alpha}$

Suppose $Z_0 = R$ and $\tau_r = 1$ ns. Then condition (A-5) gives, for $C = 60$ pF, $L = 3$ nH. Plugging into condition (A-4) gives $R = Z_0 \approx 15 \Omega$.

The capacitor discharge time $RC = 15 \times 60 \times 10^{-12} = 0.9$ ns.

B. LUMPED ANALYSIS



$$\frac{v(s)}{V_0} = \frac{1}{s} \frac{R/(1+sRC)}{sL + \frac{1}{sC_0} + \frac{R}{1+sRC}} = \frac{1}{s^3LC + s^2 \frac{L}{R} + s \left(1 + \frac{C}{C_0}\right) + \frac{1}{RC_0}} \quad (B-1)$$

$$LC \frac{v(s)}{V_0} = \frac{1}{s^3 + \frac{1}{RC} s^2 + \frac{1 + C/C_0}{LC} s + \frac{1}{RLCC_0}} \quad (B-2)$$

For critical damping this should have the form

$$LC \frac{v(s)}{V_0} = \frac{1}{(s + \alpha)^3} \quad (B-3)$$

This requires that " α " satisfy three conditions:

$$3\alpha = \frac{1}{RC} \quad (B-4)$$

$$3\alpha^2 = \frac{1 + C/C_0}{LC} \quad (B-5)$$

$$\alpha^3 = \frac{1}{RLC C_0} \quad (B-6)$$

Then

$$\boxed{\frac{v(t)}{V_0} = \frac{3}{2} \frac{1}{1 + \frac{C}{C_0}} (\alpha t)^2 e^{-\alpha t}} \quad (B-7)$$

Eliminating L and R from Equations (B-4), (B-5), and (B-6) gives $\frac{C_0}{C} = 8.$

FWHM = $\frac{3.4}{\alpha}$ = 10.2 RC which for 4 ns and C = 60 pF gives R = 6.5 Ω . Returning to conditions (B-5) and/or (B-6) we get L = 8.7 nH.

The maximum value of $\frac{v(t)}{V_0}$ occurs at $\alpha t = 2$ and is equal to 0.7.

DISTRIBUTION LIST

101	Defense Technical Info Ctr ATTN: DTIC-TCA Cameron Station (Bldg 5) 012 Alexandria, VA 22314	300 AUL/LSI 64-285 001 Maxwell AFB, AL 36112
102	Director National Security Agency ATTN: TDL 001 Fort George G. Meade, MD 20755	301 Rome Air Development Center ATTN: Documents Library (TSLD) 001 Griffiss AFB, NY 13441
103	Code R123, Tech Library DCA Defense Comm Engrg Ctr 1860 Wiegle Avenue 001 Reston, VA 22090	306 Cdr, Air Force Avionics Lab ATTN: AFAL/RWF (Mr. J. Pecqueux) 002 Wright-Patterson AFB, OH 45433
104	Defense Communications Agency Technical Library Center Code 205 (P.A. Tolovi) 002 Washington, DC 20305	307 AFGL/SULL S-29 001 HAFB, MA 01731
200	Office of Naval Research Code 427 001 Arlington, VA 22217	312 HQ, AFEWC ATTN: EST 002 San Antonio, TX 78243
205	Commanding Officer Naval Research Laboratory ATTN: Code 2627, 1409, 5270 (In Turn) 001 Washington, DC 20375	314 HQ, Air Force Systems Command ATTN: DLCA 001 Andrews AFB, Washington, DC 20331
207	Cdr, Naval Surface Weapons Ctr White Oak Laboratory ATTN: Library, Code WX-21 001 Silver Spring, MD 20910	403 Cdr, MIRCOM Redstone Scientific Info Center ATTN: Chief, Document Center 002 Redstone Arsenal, AL 35809
209	Commander (Air-5471/5473) Naval Air Systems Command 002 Washington, DC 20361	404 Crd, MIRCOM ATTN: DRSMI-RE (Mr. Pittman) 001 Redstone Arsenal, AL 35809
210	Commandant, Marine Corps HQ, US Marine Corps ATTN: Code LMC, INTS (In Turn) 001 Washington, DC 20380	405 Commander US Army Aeromedical Research Lab ATTN: Library 001 Fort Rucker, AL 36362
212	Command, Control & Comm Div. Development Center Marine Corps Dev & Educ Cmd 001 Quantico, VA 22134	406 Commandant US Army Aviation Center ATTN: ATZQ-D-MA 001 Fort Rucker, AL 36362
		407 Dir, Ballistic Missile Defense Advanced Technology Center ATTN: ATC-R, PO Box 1500 001 Huntsville, AL 35807

418	Commander HQ, Fort Huachuca ATTN: Technical Reference Div 001 Fort Huachuca, AZ 85613	476	CB Detect & Alarms Div Chemical Systems Lab ATTN: DRDAR-CLC-CR (H. Tennenbaum) 002 Aberdeen Proving Grnd, MD 21010
419	Commander US Army Electronic Proving Grnd ATTN: STEEP-MT 001 Fort Huachuca, AZ 85613	477	Dir, USA Ballistic Research Lab ATTN: DRXBD-LB 001 Aberdeen Prov Grnd, MD 21005
422	Commander US Army Yuma Proving Ground ATTN: STEYP-MTD (Tech Library) 001 Yuma, AZ 85364	481	Harry Diamond Laboratories ATTN: DELHD-R-NM (Dr. J. Nemarich) 2800 Powder Mill Road 001 Adelphi, MD 20783
433	Commander US Army STC FIO ATTN: Mr. Robert Miller 001 APO San Francisco, CA 96328	482	Director US Material Sys Anal Actv ATTN: DRXSY-T 001 Aberdeen Prov Grnd, MD 21005
437	Deputy for Science & Technology Office, Asst Sec Army (R&D) 002 Washington, DC 20310	483	Director US Material Sys Anal Actv ATTN: DRXSY-MP 001 Aberdeen Prov Grnd, MD 21005
438	HQDA (DAMA-ARZ-D/Dr. F.D. Verderame) 001 Washington, DC 20310	498	Cdr, TARADCOM ATTN: DRDTA-UL, Tech Library 001 Warren, MI 48090
455	Commandant US Army Signal School ATTN: ATSH-CD-MS-E 001 Fort Gordon, GA 30905	499	Cdr, TARCOM ATTN: DRDTA-RH 001 Warren, MI 48090
456	Commandant US Army Infantry School ATTN: ATSH-CD-MS-E 001 Fort Benning, GA 31905	503	Dir, USA Engineering Waterways Exper Station ATTN: Research Ctr Library 002 Vicksburg, MS 39108
470	Director of Combat Developments US Army Armor Center ATTN: ATZK-CD-MS 002 Fort Knox, KY 40121	507	Cdr, AVRADCOM ATTN: DRSAV-E PO Box 209 001 St. Louis, MO 63166
474	Commander USA Test & Evaluation Command ATTN: DRSTE-CT-C 001 Aberdeen Proving Grnd, MD 21005	511	Cdr, ARRADCOM ATTN: DRDAR-LOA-PD 002 Dover, NJ 07801
475	Cdr, Harry Diamond Laboratories ATTN: Library 2800 Powder Mill Road 001 Adelphi, MD 20783	512	Cdr, ARRADCOM ATTN: DRDAR-LCN-S (Bldg 95) 001 Dover, NJ 07801

513	Cdr, ARRADCOM ATTN: DRDAR-TSS, #59 001 Dover, NJ 07801	542	Commandant USAFAS ATTN: ATSF-CD-DE 001 Fort Sill, OK 73503
515	PM, FIREFINDER/REMBASS ATTN: DRCPM-FER 002 Fort Monmouth; NJ 07703	554	Commandant USA Air Defense School ATTN: ATSA-CD-MS-C 001 Fort Bliss, TX 79916
517	TRI-TAC Office ATTN: TT-SE 001 Fort Monmouth, NJ 07703	556	HQ, TCATA Technical Information Center ATTN: Mrs. Ruth Reynolds 001 Fort Hood, TX 76544
518	Cdr, USA Satellite Comm Agcy ATTN: DRCPM-SC-3 002 Fort Monmouth, NJ 07703	559	Commander USA Dugway Proving Ground ATTN: MT-T-I 001 Dugway, UT 84022
519	Cdr, USA Avionics Lab AVRADCOM ATTN: DAVAA-D 001 Fort Monmouth, NJ 07703	563	Commander, DARCOM ATTN: DRCDE 5001 Eisenhower Avenue 001 Alexandria, VA 22333
521	Cdr, Project Manager, SOTAS ATTN: DRCPM-STA 001 Fort Monmouth, NJ 07703	564	Cdr, USA Signals Warfare Lab ATTN: DELSW-OS Vint Hill Farms Station 001 Warrenton, VA 22186
528	Cdr, USA Research Office ATTN: Dr. David Squire PO Box 12211 001 Research Triangle Park, NC 27709	567	Commandant US Army Engineer School ATTN: ATZA-TDL 002 Fort Belvoir, VA 22060
529	Cdr, USA Research Office ATTN: Dr. Horst Wittmann PO Box 12211 001 Research Triangle Park, NC 27709	568	Commander USA Mobility Eqp Res & Dev Cmd ATTN: DRDME-R 001 Fort Belvoir, VA 22060
531	Cdr, USA Research Office ATTN: DRXRO-IP PO Box 12211 002 Research Triangle Park, NC 27709	569	Commander USA Engineer Topographic Labs ATTN: ETL-TD-EA 001 Fort Belvoir, VA 22060
532	Cdr, US Army Research Office ATTN: DRXRC-PH (Dr. R.J. Lontz) PO Box 12211 002 Research Triangle Park, NC 27709	571	Dir, Applied Tech Lab USA Rsch & Tech Labs (AVRADCOM) ATTN: Technical Library 001 Fort Eustis, VA 23604
533	Commandant USA Inst for Military Assistance ATTN: ATSU-CTD-MO 002 Fort Bragg, NC 28307	575	Commander, TRADOC ATTN: ATDOC-TA 001 Fort Monroe, VA 23561
537	Cdr, USA Tropic Test Center ATTN: STETC-Tech-Info Ctr 001 APO Miami 34004		

576	Commander USA Training & Doctrine Cmd ATTN: ATCD-IE 001 Fort Monroe, VA 23651	616	Cdr, ERADCOM ATTN: DRDEL-SB 2800 Powder Mill Road 001 Adelphi, MD 20783
579	PM, Control & Analysis Ctrs Vint Hill Farms Station 001 Warrenton, VA 22186	619	Cdr, ERADCOM ATTN: DRDEL-PA 2800 Powder Mill Road Adelphi, MD 20783
602	Cdr, NV&EOL, ERADCOM ATTN: DELNV-D 001 Fort Belvoir, VA 22060	620	Cdr, ERADCOM ATTN: DRDEL-I-TL 2800 Powder Mill Road Adelphi, MD 20783
603	Cdr, Atmospheric Sciences Lab ERADCOM ATTN: DELAS-SY-S 001 White Sands Missile Rng, NM 88002	680	Commander US Army Electronics R&D Command 000 Fort Monmouth, NJ 07703
604	Chief, Office of Missile Electronic Warfare Electronic Warfare Lab ERADCOM 001 White Sands Missile Rng, NM 88002		1 DRDEL-SA 1 DELEW-D 1 DELCS-D 1 DELET-DD 1 DELET-DX 1 DELSD-D 1 DELSD-L (Library) 2 DELSD-L-S (Stinfo) 25 Originating Office
606	Chief Intel Material Dev & Sup Ofc Electronic Warfare Lab ERADCOM 001 Fort Meade, MD 20755	681	Commander US Army Comm R&D Command 000 Fort Monmouth, NJ 07703
607	Cdr, Harry Diamond Labs ATTN: DELHD-CO,TD (In Turn) 2800 Powder Mill Road 001 Adelphi, MD 20783		1 DRDCO-COM-RO 1 USMC-LNO 1 ATFE-LO-EC
608	Cdr, ARRADCOM ATTN: DRDAR-TSB-S 001 Aberdeen Proving Grnd, MD 21005	682	Commander US Army Comm & Electronics Material Readiness Command 000 Fort Monmouth, NJ 07703
609	Cdr, ERADCOM ATTN: DRDEL-CG,CD,CS (In Turn) 2800 Powder Mill Road 001 Adelphi, MD 20783		1 DRSEL-PL-ST 1 DRSEL-MA-MP 1 DRSEL-PA
612	Cdr, ERADCOM ATTN: DRDEL-CT 2800 Powder Mill Road 002 Adelphi, MD 20783	701	MIT Lincoln Laboratory ATTN: Library (Rm A-082) 002 Lexington, MA 02173
615	Cdr, ERADCOM ATTN: DRDEL-SB 2800 Powder Mill Road 001 Adelphi, MD 20783	703	NASA Scientific & Tech Info Facility Baltimore/Washington Intl Airport 001 PO Box 8757, MD 21240

704 National Bureau of Standards
Bldg 225, Rm A-331
ATTN: Mr. Leedy
001 Washington, DC 20231

705 Advisory Group on Electron Devices
201 Varick Street, 9th Floor
002 New York, NY 10014

707 TACTEC
Batelle Memorial Institute
505 King Avenue
001 Columbus, OH 43201

709 Plastics Tech Eval Center
Picatinny Arsenal, Bldg 176
ATTN: Mr. A. M. Anzalone
001 Dover, NJ 07801

**DATE
ILMED
-8**